IHC_Tool: An open-source Fiji procedure for quantitative evaluation of cross sections of testicular explants

Ludovic Dumont, Nicolas Levacher, Damien Schapman, Aurélie Rives-Feraille, Laura Moutard, Marion Delessard, Justine Saulnier, Christine Rondanino, Nathalie Rives

IHC_Tool: An open-source Fiji procedure for quantitative evaluation of cross sections of testicular explants

[1,2,*]Ludovic Dumont, [3]Nicolas Levacher, [4]Damien Schapman, [1,2]Aurélie Rives-Feraille, [1,2]Laura Moutard, [1,2]Marion Delessard, [1,2]Justine Saulnier, [1,2]Christine Rondanino and [1,2]Nathalie Rives

[*]Correspondence address

Tel: +332-35-14-82-95; e-mail: ludovic.dumont1@univ-rouen.fr

EA 4308 "Gametogenesis and Gamete Quality" Laboratoire de Biologie de la Reproduction – 22 Boulevard Gambetta | UFR Santé, 76183 Rouen Cedex 1, France

Affiliations of authors:

[1] Normandie Univ, UNIROUEN, EA 4308 "Gametogenesis and Gamete Quality", Rouen University Hospital, Department of Reproductive Biology – CECOS, F 76000 Rouen, France

[2] Institute for Research and Innovation in Biomedicine (IRIB), Rouen, France

[3] OmicX | Seine Innopolis, Le-Petit-Quevilly, France

[4] Normandie Univ, UNIROUEN, INSERM, PRIMACEN, F 76000 Rouen, France

E-mail addresses of contributors:

First name	Last name	e-mail address
Ludovic	Dumont	l.dumont@live.fr
Nicolas	Levacher	nicolas.levacher@orange.fr
Damien	Schapman	damien.schapman@univ-rouen.fr
Aurélie	Rives-Feraille	A.Rives-Feraille@chu-rouen.fr
Laura	Moutard	laura.moutard@univ-rouen.fr
Marion	Delessard	marion.delessard@etu.univ-rouen.fr
Justine	Saulnier	justine.saulnier1@univ-rouen.fr
Christine	Rondanino	christine.rondanino@univ-rouen.fr
Nathalie	Rives	nathalie.rives@chu-rouen.fr

Short title: Fiji Procedure for Testicular Tissue Evaluation

ABSTRACT

Immunohistochemical analysis is a routine procedure for clinical and research studies in male fertility. However, most of the interpretations remain subjective and time-consuming, with inherent intra- and inter-observer variability. Given the prognostic and research implications of testicular assessment, a more objective and less time-consuming method is required. In the current study, we used *in vitro* matured pre-pubertal murine testes as a model. The main objective was to develop an affordable automated digital immunohistochemistry image analysis tool for an unbiased and quantitative assessment of testicular tissue sections. Testicular explants were fixed, cut, and stained for specific germ cell markers. The classical manual counting procedure was evaluated. Background and noise were reduced on brightfield images. Photomicrographs were stitched (*Background_Elimination_Stitching*) to create high-quality images. Two procedures were evaluated (*IHC_Tool* and *Stained_Nuclear_Area*); then a procedure (*Necrotic_Area_Elimination*) allowing withdrawal of the necrotic area observed after culture was assessed. Finally, the number of stained nuclei in the unaltered tissue area was extracted. The automated *IHC_Tool* procedure with images saved as TIFF at a ×200 magnification allowed the most rigorous cell quantification. *IHC_Tool* developed for testicular sample analysis can be used for various types of tissues. We foresee that this method will minimize inter-observer variations across laboratories and will be helpful for clinical trials and translational initiatives.

Keywords: Brightfield, Imaging, Immunohistochemistry, Microscopy, Testis

LIST OF ABBREVIATIONS

CF, clear field (field of a view without sample)

CREM, cAMP-responsive element modulator

CV, coefficient of variation

$\bar{d}$, nuclear 'diameter' in germ cells

DAB, diaminobenzidine (brown labeling)

DF, dark field (with the closed camera shutter)

Exam. 1, naive examiner

Exam. 2 and 3, experienced examiners

IHC, immunohistochemistry

LAS®, Leica Application Suite

1. INTRODUCTION

The diagnosis of pathology is constantly evolving, thanks to new knowledge and novel technologies that are becoming more affordable. However, each technique has its own limitations and pitfalls [1-3]. In the field of andrology, inter- and intra-investigator variations (more often between experienced and inexperienced observers) have been reported for testicular descent [4], orchidometer measurements of testicular volume [5], clinical examinations including estimation of testicular size and volume [6-7] and testicular lesions [8]. In the field of fertility preservation and restoration in childhood cancer (*e.g.*, by *in vitro* maturation of testicular explants), each team evaluate testicular tissues in their own way. The traditional immunohistochemistry (IHC) technique remains an appropriate technique to evaluate testicular tissues for patient management or research studies [9]. The expression of antigens of interest is commonly visualized using the 3,3'-Diaminobenzidine (DAB) substrate (brown staining). The analysis of tissue sections is mainly based on manual scoring, and to a lesser extent performed using computer-assisted image processing [10]. The conventional method by manual examination is considered accurate in most cases, but is also known to suffer from inter- and intra-observer variability, especially for abnormal features and tissue-handling artifacts [11]. Moreover, the brightfield intensity of immunostaining can lead to scoring decision directly influenced by visual bias, especially on damaged testicular tissue samples or *in vitro* matured testicular explants. In addition, examiners need to determine the level of precision with each run of biological assay to estimate the potential systematic and random measurement errors [12].

The rising incidence of testis cancer and carcinoma *in situ* especially in at risk subgroups such as infertile men requires strategies for early detection, ideally at the pre-invasive stage [13]. Strong discrepancies for histological testicular tissue evaluation (and the use of

78 imprecise terminology and fixation for testicular tissue) seriously degrade the value of the
79 literature [12]. The complexity of the identification of cells is mainly dependent to the
80 examiner experience (*e.g.*, initial training –clinician, scientist, technician, *etc*...–, experience
81 on the type of slides to be analyzed, time in the structure which performs the slide
82 evaluations, the quality of the training, *etc*…). The re-evaluation of testicular biopsies
83 analyses who were externalized or the comparison of results obtained in different studies
84 carried out with the same *in vitro* matured testicular explants revealed that some reports were
85 deficient and that clinical or scientific conclusions may have been improved by the use of a
86 systematized approach (internal laboratory data). Digital evaluations offers significant
87 improvement to overcome subjectivity and improve reproducibility [14]. However, images
88 are increasingly sensitive to a loss of digital information caused by a waste compression
89 algorithm (*e.g.*, JPEG) with loss of information that cannot be recovered [15]; it is therefore
90 necessary to determine the format that will be used to save the images. On the other hand, the
91 detailed analysis of tissue sections is an extremely time-consuming activity that must be
92 carried out by very experienced staff [16]. It is therefore crucial to adopt a less time-
93 consuming, more accurate and reproducible strategy capable of evaluating a large panel of
94 different parameters.

95 In the present study, histological evaluations were performed on testicular tissues from
96 mice aged 6.5 days *postpartum* and cultured for 30 days. After *in vitro* culture, testicular
97 explants were handled and germ cells were immunostained using specific antibodies and the
98 DAB chromogen. The central area, which becomes necrotic during *in vitro* culture, was
99 evaluated to obtain an accurate estimation of the quality of *in vitro* matured testicular
100 explants. The aim of the current study was to create a simple procedure – accessible to
101 clinical and research teams with basic laboratory equipment (*i.e.*, a brightfield microscope

coupled with a camera) – capable of (i) **reducing background and noise** on brightfield images, (ii) generating a global **stitched high-resolution representation** of testicular tissue sections, (iii) extracting the proportion of **necrotic area** (semi-automatically), and (iv) counting the **number of immunostained cells** per surface of unaltered area.

2. MATERIALS AND METHODS

2.1. Testicular Tissues

2.1.1. Ethical approval

Due to the scarcity of pre-pubertal human samples, this study was carried out with an animal model. The animal care and use committee of Rouen University (N/23-11-12/46/11-15) approved all the experimental procedures.

Animal care and use statement

The protocol was designed to minimize pain or discomfort to the animals. The mice were acclimatized to laboratory conditions (23°C, 12 h/12 h light/dark, and 50% humidity). Pre-pubertal 6.5-day-old CD-1 male mice (Charles River Laboratories, L'Arbresle, France) were euthanized by decapitation for tissue collection.

2.1.2. Testicular Tissue Collection and Handling

Pre-pubertal testicular testes from mice aged 6.5 days *postpartum* were cut into four fragments (0.75 mg each), cultured for 30 days under 5% CO_2 at 34°C in six-well plates (130184; Thermo Fisher Scientific Inc., Waltham, Massachusetts, USA), as previously described [17]. The culture medium was composed of α-MEM (22561-021; Gibco® by Thermo Fisher Scientific Inc), 10% (v/v) KnockOut™ serum replacement (KSR) (10828-010; Gibco®), 5 µg/mL gentamicin (G1397; Sigma-Aldrich®, Saint-Quentin-Fallavier, France) and 10^{-6} M retinol (Rol, vitamin A, all-*trans* retinol; R7632; Sigma-Aldrich®). Rol was added at D2 to initiate spermatogenesis. The medium was changed every 4 days and the supplementation with Rol was performed every 8 days to mimic the physiological timing of the seminiferous epithelium cycle.

Because the testis is a very water-rich tissue, high water content fixatives produces less shrinkage. The volume of testicular material did not change with the use of Bouin's solution [18]. Therefore, testicular tissue explants were fixed in Bouin's solution (HT10132; Sigma-Aldrich) for 2 h at RT, then dehydrated in a graded series of ethanol baths and embedded in paraffin. Sections (3 µm thick) were cut using a microtome (JungRM 2035; Leica Microsystems© GmbH, Wetzlar, Germany). Three serial tissue sections were mounted on each Polysine® slide (J2800AMNZ; Thermo Fisher Scientific Inc.). Three sections, representing the two side-ends and the middle of the sample, were examined to obtain a more accurate and global assessment of the tissue.

2.1.3. Immunohistochemistry

Testicular tissue sections were immunostained using (i) anti-TRA98, specific for spermatogonia as well as leptotene/zygotene spermatocytes I or (ii) anti-cAMP-responsive element modulator (CREM), to detect late pachytene spermatocytes I and round spermatids. For the detection of TRA98 (1:200; ab82527; Abcam®, Paris, France), tissue sections were incubated with a rabbit anti-rat secondary antibody (1:200; P0450; Dako) and subsequently with a biotinylated swine anti-rabbit tertiary antibody (1:200; E0353; Dako) plus a peroxidase-conjugated streptavidin (TP-060-HDX; Microm Microtech). CREM (clone X-12; 1:50; sc-440; Santa Cruz Biotechnology Inc., Heidelberg, Germany) was detected using a biotinylated goat anti-rabbit secondary antibody (1:200; sc-2040; Santa Cruz Biotechnology Inc.) plus a peroxidase-conjugated streptavidin. DAB (TA-060-HDX; Microm Microtech, Brignais, France) was used as a chromogen and tissues were counterstained with hematoxylin (S2020; Dako by Agilent Technologies, Santa Clara, California, USA). Negative controls were performed with rat (1:200; sc-2026; Santa Cruz Biotechnology Inc.) or rabbit (1:200; sc-2027; Santa Cruz Biotechnology Inc.) immunoglobulin G.

153 Serial digital IHC images were acquired with a light microscope (DM4000B®) equipped
154 with the Leica Application Suite (LAS®).

155 **2.2. Examiners Variation Analysis (Inter-Observer Reproducibility)**

156 Stained tissue sections were observed manually, blindly, and analyzed independently by three
157 observers to assess variations between a naive examiner (Exam. 1) and two experienced
158 examiners (Exam. 2 and 3). Exam. 1 is a Master's Degree student (6 months of internship;
159 trained in 2 months to ensure that the same criteria were used for the assessment of testicular
160 tissue staining), Exam. 2 and 3 were Ph.D. scientists (8 and 9 years of experience,
161 respectively; trained by skilled clinical histopathologists). Intra- and inter-assay variations –
162 which contribute to the overall reproducibility of a technique– were determined individually.
163 Ten iterations of the same slide were performed by each examiner on seminiferous tubules in
164 sections of testicular tissues cultured for 30 days and stained with anti-TRA98 and anti-
165 CREM antibodies.

166 Intratubular cells were classified as germ cells (brown nuclei) or Sertoli cells (irregular,
167 blue nuclei). Germ cells were identified by the examiners on TRA98-stained tissue sections
168 and classified as spermatogonia (smooth, spherical brown nuclei), leptotene / zygotene
169 spermatocytes I (irregular, spherical, brown nuclei with condensed chromatin), pachytene
170 spermatocytes I (irregular spherical brown nuclei with highly condensed chromatin), round
171 spermatids (regular, small, round blue nuclei) or elongated spermatids (elongated, blue nuclei
172 with highly condensed chromatin). Sertoli cells were in addition identified in order to check
173 whether the experience and training of the various examiners could also have a strong impact
174 on unstained cells (identified solely by their histological characteristics). Sertoli cells were
175 defined by their tall columnar shape, which spans from the basement membrane to the lumen

of seminiferous tubules. They surround the proliferating and differentiating germ cells, forming pockets around these cells.

2.3. Evaluation of Automatic Procedures and Data Processing (Digital Image Analyses)

Personal macros were written with the Fiji software [19]. Fiji as a bundle is licensed (https://github.com/fiji/fiji/blob/master/LICENSES) under the GNU General Public License (Version 3, 29 June 2007) –as specified at http://www.gnu.org/licenses/gpl.txt–, with exceptions for plugins and other components.

2.3.1. Background_Elimination_Stitching Procedure

To reduce background and noise on brightfield images, each tissue section was acquired 'field by field' at several magnifications (corresponding to a ten-eyepiece magnification combined with an objective) according to acquisition parameters to optimize the image analysis workflow. To obtain an optimal image quality obtained after stitching/analysis time ratio, the ×10, ×20, and ×50 (oil) objectives were evaluated. The image then underwent the following changes: (i) a **brightness enhancement** (min: 90, max: 250) coupled with the LUT_Editor plugin run, (ii) a **threshold** (1, 220) to eliminate the background, (iii) **morphological modifications** to fill the image in black with a succession of Dilatations (Gray Morphology; radius=2), Fill Holes, and Remove Outliers (radius=2, threshold=50), and (iv) an **erosion** (Gray Morphology; radius=6) to correct dilatations. Images (initially evaluated in pixels) were processed independently according to their magnification (corresponding to a ten-eyepiece magnification combined with ×10, ×20 or ×50 objectives):

- ×100 (unit=um; pixel_width=0.45654296875; pixel_height=0.45703125)
- ×200 (unit=um; pixel_width=0.2280273; pixel_height=0.2285156)

- ×500 (unit=um; pixel_width=0.09130859375; pixel_height=0.09114583333333333)

Images were saved as JPEG and TIFF for a Clear Field (CF, field of a view without sample) and a Dark Field (DF, with the closed camera shutter) for a normalization step. A set of background- and noise-reduced brightfield images was generated. Then, an automatic procedure recognized the overlapping points between corrected images to allow a stitching and the creation of a high-quality image of the whole tissue fragment. The macro is available at https://github.com/LudovicDumont/Background_Elimination_Stitching.git. A flowchart schematizing the processing performed by the *Background_Elimination_Stitching* procedure is shown in **Figure 1**. To compare the different conditions evaluated in this article (*i.e.*, magnification, save-file format, procedure), a relative difference between experiments was measured. The formula for this type of percent error is: *relative difference between condition A and B* = $\left| 1 - (condition\ B)/(condition\ A) \right| \times 100$.

2.3.2. Necrotic_Area_Elimination Procedure

A necrotic area appears during *in vitro* culture, making the quantification of this field irrelevant for IHC analysis. This necrotic area is composed of apoptotic cells with pyknotic nuclei (small condensed nuclei) with shrunken cytoplasm, necrotic cells, and with the formation of large vacuolizations. If the 'necrotic elimination' was ticked in the parameters presented in a dialog box at the launch of the macro, the relative proportion of the selected necrotic area (delimited by the user with the 'region of interest' tool) was calculated.

Testicular tissue explants were evaluated according to their necrotic area (μm^2), total area (μm^2) and necrotic area proportion (%). A flowchart schematizing the processing performed by the *Necrotic_Area_Elimination* procedure is shown in **Figure 2**.

2.3.3. IHC_Tool Procedure

To quantify the number of TRA98- and CREM-positive nuclei, DAB-stained elements were analyzed (min: 90, max: 250 for TRA98; min: 0, max: 205 for CREM) after (i) a selective **color deconvolution** step (Methyl Green DAB), (ii) a transformation into a **binary image** with an auto threshold (Otsu Threshold) [20], (iii) **morphological modifications** to suppress smallest elements considered as artifacts with a succession of Mask formation, Remove Outliers (radius=2.5 then 5, threshold=50), specific staining Remove Outliers (radius=7.5 for TRA98; radius=12 for CREM), Fill Holes, Dilatations, (iv) an **erosion** to correct dilatations, and (v) a **segmentation** process (Watershed Procedure) to separate adjacent structures by making bigger regions from groups of low intensity pixels (*i.e.*, germs) (**Figure 3**). Only structures with a circularity between 0.50 and 1.00 were kept. The final data that will be extracted by this procedure are the number of specifically stained nuclei (*i.e.*, TRA98- and CREM-positive) and the number of positive cells per 1000 µm^2 of tissue. A macro combining *Background_Elimination_Stitching*, *Necrotic_Area_Elimination*, and *IHC_Tool* procedures is available at https://github.com/LudovicDumont/IHC-Tool.git.

2.3.4. Stained_Nuclear_Area Procedure

In order to have numerical data corresponding to the cells present on the sections provided, the nuclear 'diameter' ($\bar{d}$) of germ cells was manually measured at right angle in the section plane to quantify the area (approximated to $\pi \times \bar{d}^2 : 4$) of TRA98- and CREM-positive cell nuclei. A total number of 100 cell nuclei were counted per group (**Supplementary Figure 1**).

To quantify the number of TRA98- and CREM-positive nuclei, the total intensity of DAB-stained elements was reported to the estimated size of the corresponding cells according to the staining (spermatogonia and leptotene-zygotene spermatocytes I for TRA98 or late pachytene spermatocytes I and round spermatids for CREM). The final extracted data are considered to be the number of positive cells per 1000 µm^2 of unaltered area.

2.4. Statistical Analyses

Statistical analyses were performed with GraphPad Prism version 6.00 (GraphPad Software, La Jolla, California). The Mann-Whitney test was used for unpaired rank comparisons and the nonparametric unilateral one-tailed Wilcoxon test was used for paired rank comparisons. The one-way ANOVA test was used for the evaluation of assays reproducibility, followed by a multiple comparison. The ordinary two-way ANOVA test was used for the evaluation of the testicular tissue analyses, followed by a Tukey's multiple comparison post-hoc test. Data are presented as means ± SEM and $P<0.05$ was considered to be significant.

3. RESULTS

3.1. Manual Analysis by Examiners is Hardly Reproducible

During the manual evaluation of *in vitro* matured testicular explants, Exam. 1 overestimated the number of leptotene-zygotene spermatocytes I (12.6±3.02 cells) compared to Exam. 2 (7.22.2±3.68 cells, P=0.0462) (**Figure 4A**). This discrepancy may be explained by the difficulty of distinguishing spermatogonia from leptotene-zygotene spermatocytes I, which are both TRA98-labelled. In addition, we observed a wide disparity between the manual evaluations made by naïve Exam. 1 and experienced Exam. 2 and Exam. 3 (**Figure 4B**). On the other hand, experienced Exam. 2 and Exam. 3 have very tight confidence intervals for all quantified cell types. In addition, a strong correlation (y=0.8887x+0.6394; R^2=0.9873, P<0.0001) was found between Exam. 2 and 3 (**Figure 4B**), confirming that a good observation training is required in order to have repeatable and comparable manual evaluation results between examiners. Finally, a Bland-Altman plot analysis carried out to assess the reliability between the readings of the different observers confirms the above findings (**Supplementary Figure 2**).

Intra-assays for the count of spermatogonia were considered to be too high for naïve Exam. 1 (1.30-13.6%; CV=28.8%). Indeed, approval limit variations of the U.S. Food and Drug Administration and the European Medicines Agency for intra-assay signal (~10 and 6-13%, respectively) were not respected, suggesting that repetitive manual evaluations of tissue sections can affect the reproducibility if the examiner is not well trained enough. The same conclusions were reached to a lesser extent for inter-examiner assays corresponding to the count of spermatogonia and Sertoli cells between Exam. 1 and Exam. 2 & Exam. 3. The variations in the approval limits for inter-assay signals were ~20 and 7-14%, respectively. For

all these reasons and in order to have reference values, data obtained by experienced Exam. 2 were compared to automated analyses.

Regarding the semi-automated evaluation of the necrotic area, the examiners had no problems in its determination. There is some heterogeneity in the testicular explant sections, however the evaluation of the proportion of necrotic area to total area was similar between the different examiners (**Supplementary Figure 3**).

3.2. Validation of the *Background_Elimination_Stitching* Procedure

CF (**Figure 5A$_1$**) and DF (**Figure 5A$_2$**) were used on original images (**Figure 5A$_3$**) for a normalization step to generate corrected images (**Figure 5A$_4$**). The mean grey values – corresponding to the background noise – were lower for corrected (2.41 ± 0.56) than for original (16.7 ± 2.12; P=0.0020) images (**Figure 5A$_5$**), validating the *Background_Elimination* procedure. Aside, the *Stitching* procedure allowed the gathering of a batch of images, leading to the building of a single high-quality image (**Figure 5B**). Altogether, these results validate the *Background_Elimination_Stitching* procedure.

3.3. Evaluation of Automatic Procedures and Data Processing

3.3.1. The IHC_Tool Procedure is Superior to the Stained_Nuclear_Area Procedure

The relative difference observed for *IHC_Tool* TIFF ×100 (42.3 ± 11.5%) was lower than for *Stained_Nuclear_Area* TIFF ×100 (121 ± 24.5%; P<0.0001) (**Figure 5C**). In addition, *IHC_Tool* TIFF ×200 (3.92 ± 0.92%) showed a better profile compared to *Stained_Nuclear_Area* TIFF ×200 (46.6 ± 21.8%; P=0.0268).

3.3.2. TIFF and JPEG formats are equivalent, except for Stained_Nuclear_Area ×100

299 *Stained_Nuclear_Area* TIFF ×100 (121 ± 25.5%) showed a poorer profile compared to
300 *Stained_Nuclear_Area* JPEG ×100 (46.6 ± 14.6%; P<0.0001) (**Figure 5C**). However, no
301 difference was observed between TIFF and JPEG formats for *IHC_Tool*. In addition, the time
302 duration for the *IHC_Tool* computerized procedure, which depends on the number of original
303 images for uncompressed and heavier TIFF images (y=38.282x–170.77; R^2=0.90493), was
304 not longer compared to JPEG images (y=38.506x–164.99; R^2=0.91324). Before the image
305 processing starts, the run duration will be estimated and presented to the users according to
306 the magnification used for image acquisition, the save-file format, and the number of images
307 to be compiled.

308 *3.3.3. Magnifications at ×200 and ×500 are better than at ×100*

309 The relative difference observed for *IHC_Tool* TIFF ×100 (42.3 ± 11.5%) was higher
310 than for *IHC_Tool* TIFF ×200 (3.92 ± 0.92%; P=0.0306) and *IHC_Tool* TIFF ×500
311 (4.62 ± 1.92%; P=0.0342) (**Figure 5C**). Moreover, *Stained_Nuclear_Area* TIFF ×100
312 (121 ± 25.5%) showed a poorer profile compared to *Stained_Nuclear_Area* TIFF ×200
313 (46.6 ± 21.8%; P<0.0001) and *Stained_Nuclear_Area* TIFF ×500 (19.7 ± 9.60%; P<0.0001).

314 **3.4. Selection of the Adapted Automatic Procedure**

315 *IHC_Tool* TIFF ×200 and *IHC_Tool* TIFF ×500 were considered to be the two best
316 procedures. Considering that a procedure performed at a ×500 magnification requires an
317 acquisition time approximately three times longer than at a ×200 magnification, the *IHC_Tool*
318 TIFF ×200 procedure from stitched samples was selected as the best strategy for evaluating
319 IHC on *in vitro* cultured testicular tissue. A summary diagram of the whole procedure (from
320 an image generated with the *Background_Elimination_Stitching*) is available in **Figure 6**.
321 Nevertheless, the choice of the save-file format remains preserved and magnifications

322 corresponding to ×5, ×10, ×20, ×40, and ×50 objectives were added into the macro to allow
323 an adaptation for next users.

324

4. DISCUSSION

Achieving a common consensus in the quantitative analysis of immunohistochemical images is still an issue in various clinical or translational researches [21]. Testis biopsy with diagnostic and prognostic importance is a crucial assessment in reproductive practice in the evaluation of men at risk [22]. For an accurate histological classification, proper tissue handling, fixation, preparation of the specimen and evaluation are needed [23]. Re-evaluation of testis biopsies reported externally often reveals that the original report was deficient and that clinical care may have been improved by the use of a systematized approach.

In the present study, we showed that manual examination is hardly reproducible. Herein, we focused on the development of a series of macros for an open-source image processing package based on ImageJ to quantify staining of IHC images, which requires minimal supervision for analysis. The establishment of procedures is an example of the initiative of the collaborative effort between computational biology and research engineering, showing the usefulness of teaching computer programming elements [24]. The amount of tissue analyzed is respectable and provides a good evaluation of the different computational tools proposed. Moreover, as the first part of the study is focused on intra- and inter-observer variability of the different examiners, the number of replicates studied was largely sufficient. The evaluation of the necrotic part turned out to be very simple, even for a novice examiner. However, some disparity between the tissue sections were observed. This may be due to the fact that the necrotic area forms in the core of the tissue explant and that the exact location and orientation of the tissue explants during inclusion remains difficult to standardize.

In this study, with the *IHC_Tool* procedure at a ×200 magnification and a backup in TIFF format, we (i) reduced background and noise on brightfield images, (ii) generated a global stitched high-resolution representation of testicular tissue sections, (iii) extracted the

proportion of necrotic area, and (iv) allowed an automated counting of the number of immunostained cells per 1000 µm^2 of unaltered area. These IHC evaluations were consistent with other studies carried out by our team on *in vitro* matured testicular explants for the number of immunostained nuclei [17, 25-30] and the proportion of necrotic area [17, 25].

The procedures developed in this study are running on Fiji software, which creates a 'profile analysis' of a digital IHC image. The selected procedure offers many advantages: (i) is compatible with an open-source and widely used digital image analysis Fiji program unlike a few tools that require a separate platform to perform the desired operation; (ii) requires only the original image photomicrographs and returns an entire corrected stitched image; (iii) eliminates inter-examiner perception bias; (iv) improves the throughput by reducing the time burden of high volume sample analysis compared to traditional manual examination; (v) remains simple, requiring only a couple of steps to analyze each sample; and (vi) reduces the severe dependency on trained clinical histopathologists.

We foresee that this method will minimize the inter-examiner variations and further help groups to use open-source software, providing a collaborative option for image analysis whereas commercial software provides more personalized image analysis choices. Each option presents certain advantages and disadvantages; a comparison between the selected *IHC_Tool* procedure, a 'generic' commercial software, and the manual examination is available in **Table 1**. This tool can be used as a systematic procedure providing crucial clinical information on the status of highly heterogeneous immature human testicular tissues in the context of cryopreservation for fertility preservation (*i.e.*, absolute germ cell numbers per area) [31]. Moreover, we provide the code of the macros validated herein, encouraging other researchers to adapt and change key elements to their specific needs like file format (*e.g.*, PNG, BMP), cell staining, magnification, morphological modifications, *etc*… In order

to improve the *IHC_Tool* procedure, it will be possible to quantify the intensity of nuclear staining in individual cells in addition to their area. The accuracy of deep learning in the field of histopathology [32] should be analyzed in detail.

This study demonstrates the development and the utility of an open-source, Fiji-compatible, and adaptable procedure towards automated quantitative analysis of testicular tissue. The *IHC_Tool* procedure analysis demonstrated high confidence with classical manual counting. We thus conclude that this method holds the potential to develop fast analyses of IHC slides for various clinical and research laboratories, minimizing inter-observer discrepancies. Moreover, this procedure developed for the analysis of testicular tissue samples can be applied for a wide variety of tissues and be used to evaluate the expression of many other proteins.

5. ACKNOWLEDGEMENTS

This work was supported by Rouen University Hospital, Ligue contre le Cancer [to N.R.], Agence de la Biomédecine [to N.R.], Association Laurette Fugain [to N.R. and C.R.], France Lymphome Espoir [to N. R.], and co-supported by European Union and Région Normandie. Europe gets involved in Normandie with European Regional Development Fund (ERDF).

6. AUTHORS' CONTRIBUTIONS

L.D.: conception and design of experiments, acquisition, analysis and interpretation of data, statistics, writing of the manuscript and final approval of the version to be published. N.L.: writing of Fiji macros and helpful assistance in immunohistochemistry combined with an automatic evaluation procedure. D.S., provided advices for Fiji macros and revision of the manuscript. A.R.F., L.M., M.D., and J.S.: provided advices during the interpretation of data. C.R.: provided advices during the conception of experiments, discussion of the results and revision of the manuscript. N.R.: conception of the research, responsible for revision and critical review of the manuscript.

7. DATA SHARING STATEMENT

Macros available at https://github.com and dataset available from the corresponding author at ludovic.dumont1@univ-rouen.fr. Participants gave informed consent for data sharing.

8. CONFLICT OF INTEREST

407 The authors declare that there is no conflict of interest.

9. FIGURES AND TABLES

9.1. Figure 1. Flowchart schematizing the image processing performed by the *Background_Elimination+Stitching* procedure.

9.2. Figure 2. Flowchart schematizing the image processing performed by the *Necrosis_Area* procedure.

9.3. Figure 3. Flowchart schematizing the image processing performed by the *IHC_Tool* procedure.

9.4. Figure 4. Comparison of manual cell counting between examiners.

(**A**) Cell type counts between the three examiners. Some values, represented by a black symbol (♦, for leptotene-zygotene spermatocyte I; ▲, for round spermatids; ■, for elongated spermatids), have been visually discarded because they are considered too far apart. **P*<0.01 between examiners 1 and 2. (**B**) Confidence intervals between examiners for cell counts. (**C**) Correlation coefficient for comparisons between examiners.

Exam., examiner.

9.5. Figure 5. Image correction, stitching of immunohistochemical images and selection of an automated procedure. (**A**) Background elimination has been developed with the use of a Clear Field (CF; $\mathbf{A_1}$) and a Dark Field (DF; $\mathbf{A_2}$). The Original Image ($\mathbf{A_3}$) represents a portion of a section of an *in vitro* matured mouse testicular tissue, stained for TRA98 (brown

DAB staining). This image sample was corrected with the CF – corresponding to a field of the slide without any sample – and the DF, corresponding to the image obtained with the closed shutter. Magnification ×200; scale bar: 50 µm. The images obtained after correction have less mean grey values (corresponding to the noise) than original images (**A**$_5$). $^{**}P<0.01$. A selection of corrected images was stitched to obtain a complete representation of the testicular tissue section (**B**). (**C**) Comparison of automated measurements obtained with *IHC_Tool* (internal Fiji macro) and *Stained_Nuclear_Area* (total staining intensity on mean nuclear size of germ cells) to manual observations. Relative differences between procedures and manual observations correspond to the absolute ratio of the number of automated counted cells obtained with the tested procedure on the value obtained with the selected manual observation. Tissues were observed under a ×100 magnification (black bars), ×200 magnification (grey bars) and ×500 magnification (white bars) and images were saved as TIFF and JPEG formats. Results are presented as means ± SEM with n=6 (each with three sections of four fragments per condition). Letters a, b, c, and d represent statistically significant differences between the corresponding tested protocols. $^{*}P<0.05$ and $^{****}P<0.0001$ between the corresponding magnifications. (**D**) Evaluation of the time duration of the *IHC_Tool* procedure between TIFF and JPEG formats.

CF, Clear Field; DAB, 3,3'-Diaminobenzidine chromogen; DF, Dark Field; SEM, standard error of the mean.

9.6. Figure 6. Schematic representation of the automated *IHC_Tool* counting procedure.

From the corrected stitched sample (**a**), the total area of the testicular tissue section was extracted by a succession of Mask, Dilate, Fill Holes, Remove Outliers and Erode processes (**b**$_1$-**b**$_5$). With a semi-automated procedure, the necrotic area generated during *in*

454 *vitro* cultures was delimitated, quantified and eliminated (**c_1-c_3**). The results of 16 bit images
455 were in white [255] to comply with the concept of "binary image" (*i.e.*, 8 bits with 0 and
456 255 values). Besides, the original color image (in RGB) was deconvoluted according to the
457 Methyl Green DAB procedure, allowing the extraction of 3 images corresponding to the
458 3 colors of interest (**d_1-d_3**). After correction of the brown image (**d_2**) and transformation to a
459 binary image (**e**), a watershed processing was applied (**f_{1-2}**), allowing the separation of
460 contiguous nuclei (red arrows).

9.9. TABLE

Procedure Name	Pros	Cons
***IHC_Tool* procedure**	• Freely available • Open-source, ImageJ2 and Fiji compatible • Bias-free analysis • Digital images can be analyzed sideways, freeing time to work on other tasks • Take about 10~15 min to analyze an image depending on the magnification, the save file format and the area studied • Easy to learn and user-friendly • Compatible (TIFF and JPEG) and extendable (*e.g.*, PNG, BMP, *etc*…) to various Original Images file formats • Runs on a multitude of operating systems (*e.g.*, Windows 32- or 64-bits [Microsoft], macOS [Macintosh; Apple Inc.], Linux 32- or 64-bits, and even without Java Runtime Environment) • Allows images to be saved and analyzed *a posteriori* • Evolutive and sharable (encouraging other researchers to adapt and change key elements to their specific needs) • Possibility to remove a 'ROI' from the analysis (*e.g.*, necrotic area)	• Does not yet have a morphometric analysis system • Cannot (as it stands) quantify fluorescent images • Can analyze, as it stands, only nuclear immunostaining • Results are saved on a local database and statistical analyses & plots have to be generated manually
Commercial Software	• Bias-free analysis • Digital images can be analyzed sideways, freeing time to work on other tasks • Take about several minutes to scan and analyze a 'ROI' on an image depending on the magnification and the area studied • Possibility to remove a 'ROI' from the analysis (*e.g.*, necrotic area) • Most often allows to analyze the morphometry • Results are stored in a Workstation database and, sometimes, statistical analyses and plots can be automatically generated	• Commercial (cost-effective) which often requires a whole slide scanner • Additional cost for purchasing apps to specific wishes • Settings often blocked or difficult to change • Specific images file formats (making recording and reading of images dependent on the private software • Runs on a specific operating system (*e.g.*, Windows [Microsoft] or macOS [Macintosh; Apple Inc.]) • May require an expert opinion for some application • Requires dedicated learning time and customer support
Manual examination	• Requires no dedicated computer system and can be performed directly	• Total time analysis >90 min • Long learning curve • Difficult to have good reproducibility (inter- and intra-individual)

Table 1. Comparison between the selected *IHC_Tool* procedure, commercial software, and manual examination.

10. REFERENCES

[1] Kim S-W, Roh J, Park C-S. Immunohistochemistry for Pathologists: Protocols, Pitfalls, and Tips. J Pathol Transl Med. 2016;50:411-418. doi: 10.4132/jptm.2016.08.08

[2] Miller RT. Avoiding pitfalls in diagnostic immunohistochemistry-important technical aspects that every pathologist should know. Semin Diagn Pathol. 2019;36:312-335. doi: 10.1053/j.semdp.2019.05.002

[3] Sun L, Pfeifer JD. Pitfalls in molecular diagnostics. Semin Diagn Pathol. 2019;36:342-354. doi: 10.1053/j.semdp.2019.06.002

[4] Wit JM, Delemarre-van der Waal HA, Faber JA, Van den Brande JL. Intra- and inter-observer variability in the assessment of testicular descent. Andrologia. 1987;19:585-90. doi: 10.1111/j.1439-0272.1987.tb01905.x

[5] Tatsunami S, Matsumiya K, Tsujimura A, Itoh N, Sasao T, Koh E, Maeda Y, Eguchi J, Takehara K, Nishida T, Miyano S, Tabata C, Iwamoto T. Inter/intra investigator variation in orchidometric measurements of testicular volume by ten investigators from five institutions. Asian J Androl. 2006;8:373-8. doi: 10.1111/j.1745-7262.2006.00143.x

[6] Carlsen E, Andersen AG, Buchreitz L, Jørgensen N, Magnus O, Matulevicuus V, Nermoen I, Petersen JH, Punab M, Suominen J, Zilaitiene B, Giwercman A. Inter-observer variation in the results of the clinical andrological examination including estimation of testicular size. Int J Androl. 2000;23:248-53. doi: 10.1046/j.1365-2605.2000.00240.x

[7] Welliver C, Cardona-Grau D, Elebyjian L, Feustel PJ, Kogan BA. Surprising interobserver and intra-observer variability in pediatric testicular ultrasound volumes. J Pediatr Urol. 2019;15:386.e1-386.e6. doi: 10.1016/j.jpurol.2019.04.016

[8] Lung PFC, Fang C, Jaffer OS, Deganello A, Shah A, Hedayati V, Obaro A, Yusuf GT, Huang DY, Sellars ME, Quinlan DJ, Sidhu PS. Vascularity of Intra-testicular Lesions:

Inter-observer Variation in the Assessment of Non-neoplastic Versus Neoplastic Abnormalities After Vascular Enhancement With Contrast-Enhanced Ultrasound. Ultrasound Med Biol. 2020;46:2956-2964. doi: 10.1016/j.ultrasmedbio.2020.07.028

[9] Bilinska B, Hejmej A, Kotula-Balak M. Preparation of Testicular Samples for Histology and Immunohistochemistry. Methods Mol Biol. 2018;1748:17-36. doi: 10.1007/978-1-4939-7698-0_3

[10] Walker RA. Quantification of immunohistochemistry--issues concerning methods, utility and semiquantitative assessment I. Histopathology. 2006;49:406-410. doi: 10.1111/j.1365-2559.2006.02514.x

[11] McLachlan RI, Rajpert-De Meyts E, Hoei-Hansen CE, de Kretser DM, Skakkebaek NE. Histological evaluation of the human testis--approaches to optimizing the clinical value of the assessment: mini review. Hum Reprod. 2007;22:2-16. doi: 10.1093/humrep/del279

[12] Kirkegaard T, Edwards J, Tovey S, McGlynn LM. Observer variation in immunohistochemical analysis of protein expression, time for a change? Histopathology. 2006;48:787-794. doi: 10.1111/j.1365-2559.2006.02412.x

[13] Cheng L, Albers P, Berney DM, Feldman DR, Daugaard G, Gilligan T, Looijenga LHJ. Testicular cancer. Nat Rev Dis Primers. 2018 Oct 5;4(1):29. doi: 10.1038/s41572-018-0029-0. PMID: 30291251.

[14] Al-Janabi S, Huisman A, Van Diest PJ. Digital pathology: current status and future perspectives. Histopathology. 2012;61:1-9. doi: 10.1111/j.1365-2559.2011.03814.x

[15] García-Rojo M. International Clinical Guidelines for the Adoption of Digital Pathology: A Review of Technical Aspects. Pathobiology. 2016;83:99-109. doi: 10.1159/000441192

[16] Giudice MG, de Michele F, Poels J, Vermeulen M, Wyns C. Update on fertility restoration from prepubertal spermatogonial stem cells: How far are we from clinical practice? Stem Cell Res. 2017;21:171-177. doi: 10.1016/j.scr.2017.01.009

514 [17] Dumont L, Chalmel F, Oblette A, Berby B, Rives A, Duchesne V, Rondanino C, Rives
515 N. Evaluation of apoptotic- and autophagic-related protein expressions before and after
516 IVM of fresh, slow-frozen and vitrified pre-pubertal mouse testicular tissue. Mol Hum
517 Reprod. 2017;23:738-754. doi: 10.1093/molehr/gax054
518 [18] Cabrera NC, Espinoza JR, Vargas-Jentzsch P, Sandoval P, Ramos LA, Aponte PM.
519 Alcohol-based solutions for bovine testicular tissue fixation. J Vet Diagn Invest. 2017
520 Jan;29(1):91-99. doi: 10.1177/1040638716672252
521 [19] Schindelin J, Arganda-Carreras I, Frise E, Kaynig V, Longair M, Pietzsch T, Preibisch
522 S, Rueden C, Saalfeld S, Schmid B, et al. Fiji: an open-source platform for biological-
523 image analysis. Nat Methods. 2012;9:676-682. doi: 10.1038/nmeth.2019
524 [20] Otsu N. A threshold selection method from gray-level histograms. IEEE Trans Syst Man
525 Cybern C Appl Rev. 1979;9:66-66. doi: 10.1109/TSMC.1979.4310076
526 [21] O'Hurley G, Sjöstedt E, Rahman A, Li B, Kampf C, Pontén F, Gallagher WM, Lindskog
527 C. Garbage in, garbage out: a critical evaluation of strategies used for validation of
528 immunohistochemical biomarkers. Mol Oncol. 2014;8:783-798. doi:
529 10.1016/j.molonc.2014.03.008
530 [22] McLachlan RI, Rajpert-De Meyts E, Hoei-Hansen CE, de Kretser DM, Skakkebaek NE.
531 Histological evaluation of the human testis--approaches to optimizing the clinical value
532 of the assessment: mini review. Hum Reprod. 2007 Jan;22(1):2-16. doi:
533 10.1093/humrep/del279. Epub 2006 Aug 3. PMID: 16887924.
534 [23] Dohle GR, Elzanaty S, van Casteren NJ. Testicular biopsy: clinical practice and
535 interpretation. Asian J Androl. 2012 Jan;14(1):88-93. doi: 10.1038/aja.2011.57. Epub
536 2011 Dec 12. PMID: 22157985; PMCID: PMC3735160.

537 [24] Brain S, Dewhurst DG, Williams AD. Evaluation of the usefulness of a computer-based
538 learning program to support student learning in pharmacology. ALT-J. 2016;7:37-45.
539 doi: 10.1080/0968776990070205
540 [25] Travers A, Arkoun B, Safsaf A, Milazzo JP, Absyte A, Bironneau A, Perdrix A, Sibert
541 L, Macé B, Cauliez B, Rives N. Effects of vitamin A on in vitro maturation of pre-
542 pubertal mouse spermatogonial stem cells. PLoS One. 2013;8:e82819. doi:
543 10.1371/journal.pone.0082819
544 [26] Dumont L, Arkoun B, Jumeau F, Milazzo JP, Bironneau A, Liot D, Wils J, Rondanino
545 C, Rives N. Assessment of the optimal vitrification protocol for pre-pubertal mice testes
546 leading to successful in vitro production of flagellated spermatozoa. Andrology.
547 2015;3:611-625. doi: 10.1111/andr.12042
548 [27] Dumont L, Oblette A, Rondanino C, Jumeau F, Bironneau A, Liot D, Duchesne V, Wils
549 J, Rives N. Vitamin A prevents round spermatid nuclear damage and promotes the
550 production of motile sperm during in vitro maturation of vitrified pre-pubertal mouse
551 testicular tissue. Mol Hum Reprod. 2016;22:819-832. doi: 10.1093/molehr/gaw063
552 [28] Arkoun B, Dumont L, Milazzo JP, Rondanino C, Bironneau A, Wils J, Rives N. Does
553 soaking temperature during controlled slow freezing of pre-pubertal mouse testes
554 influence course of in vitro spermatogenesis? Cell Tissue Res. 2016;364:661-674. doi:
555 10.1007/s00441-015-2341-2
556 [29] Arkoun B, Dumont L, Milazzo JP, Way A, Bironneau A, Wils J, Macé B, Rives N.
557 Retinol improves in vitro differentiation of pre-pubertal mouse spermatogonial stem cells
558 into sperm during the first wave of spermatogenesis. PLoS One. 2015;10:e0116660. doi:
559 10.1371/journal.pone.0116660. Erratum in: PLoS One. 2015;10:e0123846
560 [30] Rondanino C, Maouche A, Dumont L, Oblette A, Rives N. Establishment, maintenance
561 and functional integrity of the blood-testis barrier in organotypic cultures of fresh and

562 frozen/thawed prepubertal mouse testes. Mol Hum Reprod. 2017;23:304-320. doi:
563 10.1093/molehr/gax017
564 [31] Heckmann L, Langenstroth-Röwer D, Pock T, Wistuba J, Stukenborg JB, Zitzmann M,
565 Kliesch S, Schlatt S, Neuhaus N. A diagnostic germ cell score for immature testicular
566 tissue at risk of germ cell loss. Hum Reprod. 2018 Apr 1;33(4):636-645. doi:
567 10.1093/humrep/dey025. PMID: 29452353
568 [32] Jones AD, Graff JP, Darrow M, Borowsky A, Olson KA, Gandour Edwards R, Datta
569 Mitra A, Wei D, Gao G, Durbin Johnson B, et al.. Impact of pre-analytical variables on
570 deep learning accuracy in histopathology. Histopathology. 2019;75:39-53. doi:
571 10.1111/his.13844

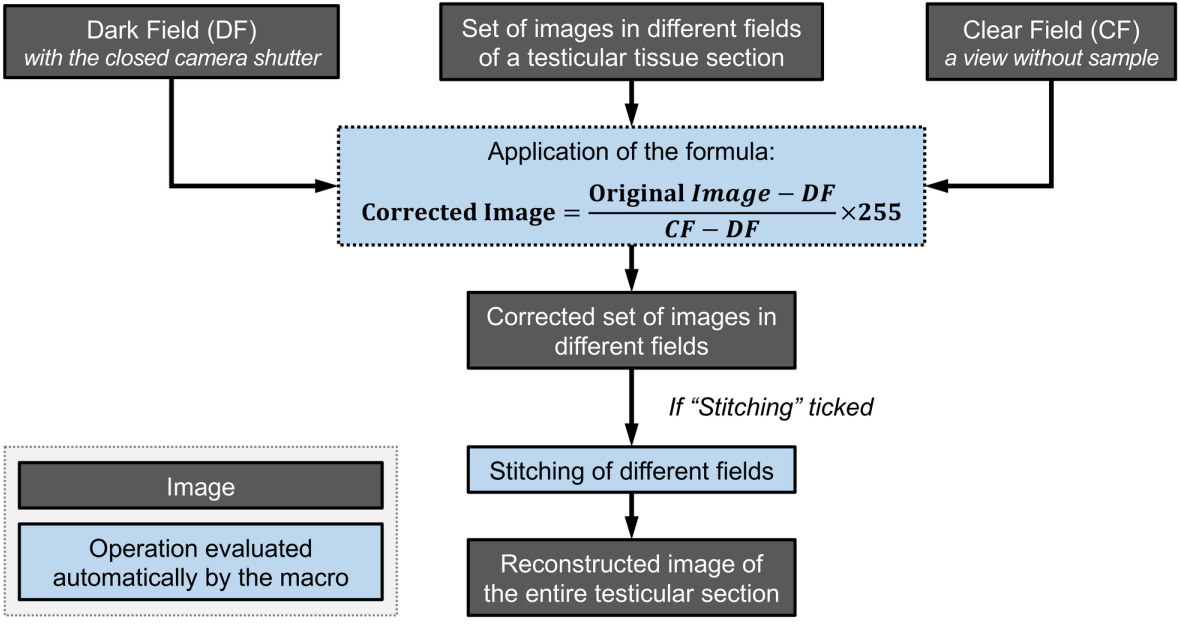
Dark Field (DF)
with the closed camera shutter
Set of images in different fields of a testicular tissue section
Clear Field (CF)
a view without sample
Application of the formula:
Corrected Image = (Original Image − DF) / (CF − DF) ×255
Corrected set of images in different fields
If "Stitching" ticked
Stitching of different fields
Reconstructed image of the entire testicular section
Image
Operation evaluated automatically by the macro

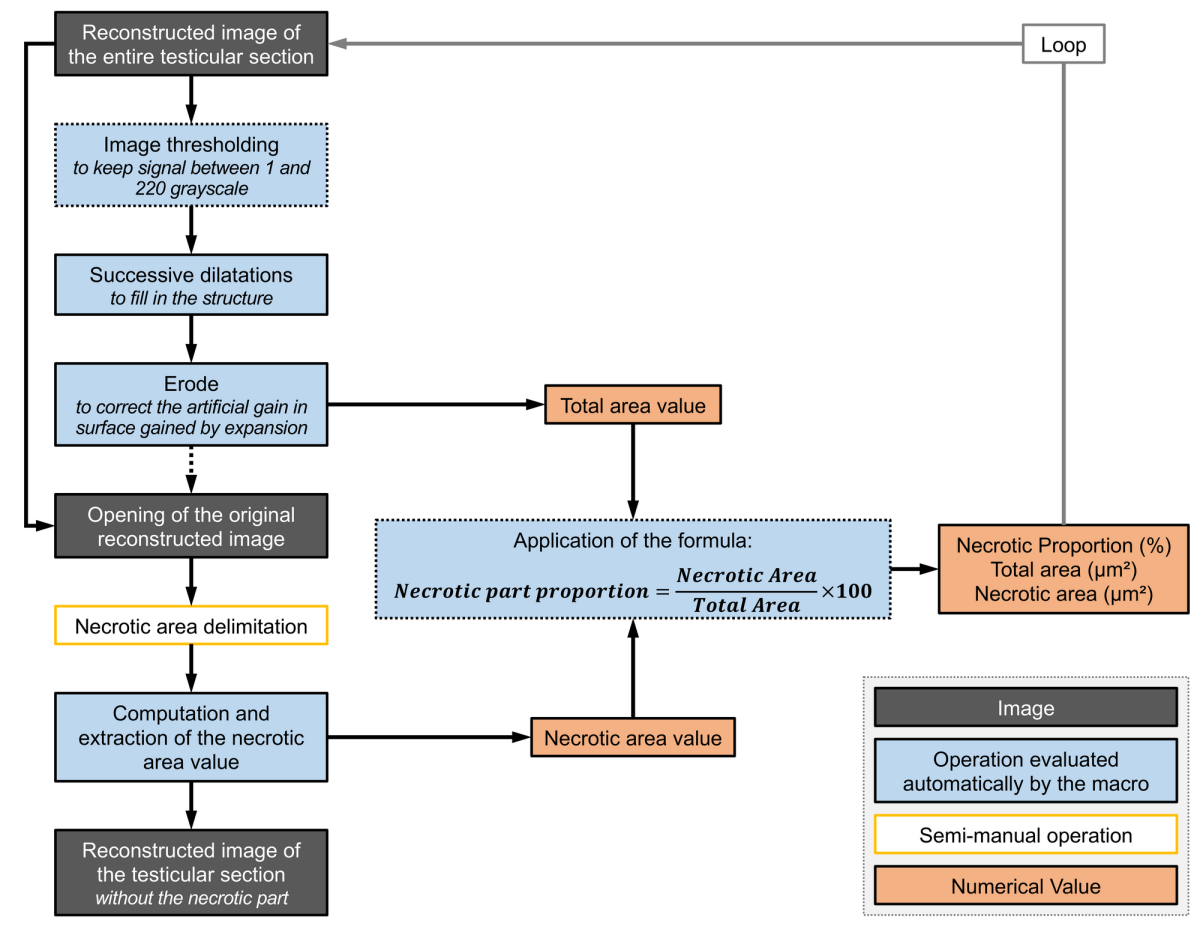
Reconstructed image of the entire testicular section
Loop
Image thresholding
to keep signal between 1 and 220 grayscale
Successive dilatations
to fill in the structure
Erode
to correct the artificial gain in surface gained by expansion
Total area value
Opening of the original reconstructed image
Application of the formula:
$Necrotic\ part\ proportion = \frac{Necrotic\ Area}{Total\ Area} \times 100$
Necrotic Proportion (%)
Total area (µm²)
Necrotic area (µm²)
Necrotic area delimitation
Computation and extraction of the necrotic area value
Necrotic area value
Reconstructed image of the testicular section
without the necrotic part
Image
Operation evaluated automatically by the macro
Semi-manual operation
Numerical Value

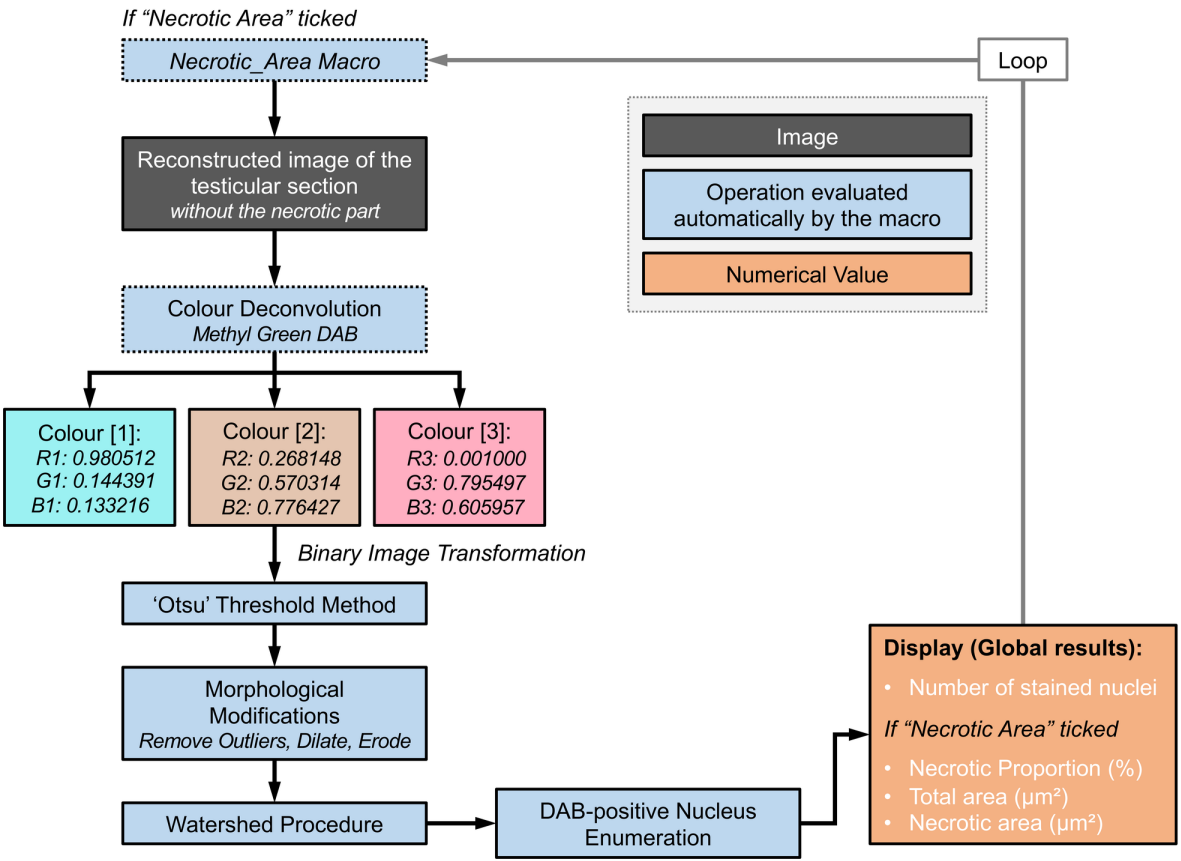
If “Necrotic Area” ticked
Necrotic_Area Macro
Loop
Image
Operation evaluated automatically by the macro
Numerical Value
Reconstructed image of the testicular section
without the necrotic part
Colour Deconvolution
Methyl Green DAB
Colour [1]:
R1: 0.980512
G1: 0.144391
B1: 0.133216
Colour [2]:
R2: 0.268148
G2: 0.570314
B2: 0.776427
Colour [3]:
R3: 0.001000
G3: 0.795497
B3: 0.605957
Binary Image Transformation
‘Otsu’ Threshold Method
Morphological Modifications
Remove Outliers, Dilate, Erode
Watershed Procedure
DAB-positive Nucleus Enumeration
Display (Global results):
• Number of stained nuclei
If “Necrotic Area” ticked
• Necrotic Proportion (%)
• Total area (µm²)
• Necrotic area (µm²)

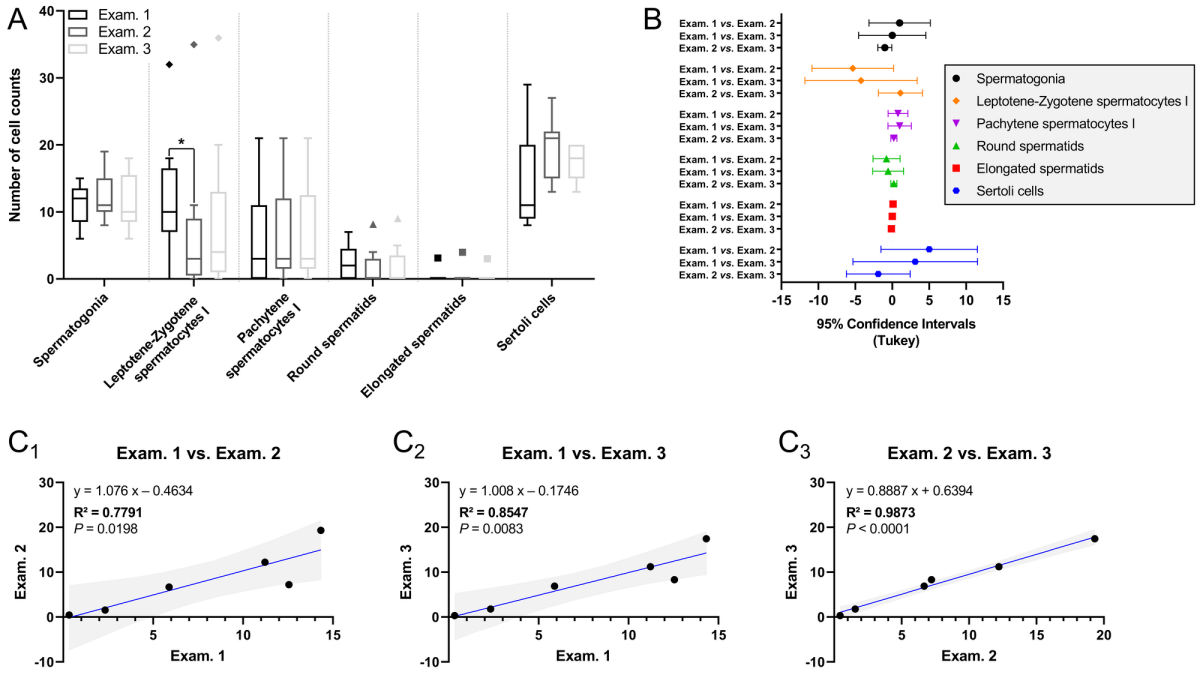
A
Exam. 1
Exam. 2
Exam. 3
Number of cell counts
40
30
20
10
0
*
Spermatogonia
Leptotene-Zygotene spermatocytes I
Pachytene spermatocytes I
Round spermatids
Elongated spermatids
Sertoli cells
B
Exam. 1 vs. Exam. 2
Exam. 1 vs. Exam. 3
Exam. 2 vs. Exam. 3
Spermatogonia
Leptotene-Zygotene spermatocytes I
Pachytene spermatocytes I
Round spermatids
Elongated spermatids
Sertoli cells
-15 -10 -5 0 5 10 15
95% Confidence Intervals (Tukey)
C1
Exam. 1 vs. Exam. 2
y = 1.076 x – 0.4634
R² = 0.7791
P = 0.0198
Exam. 2
Exam. 1
C2
Exam. 1 vs. Exam. 3
y = 1.008 x – 0.1746
R² = 0.8547
P = 0.0083
Exam. 3
Exam. 1
C3
Exam. 2 vs. Exam. 3
y = 0.8887 x + 0.6394
R² = 0.9873
P < 0.0001
Exam. 3
Exam. 2

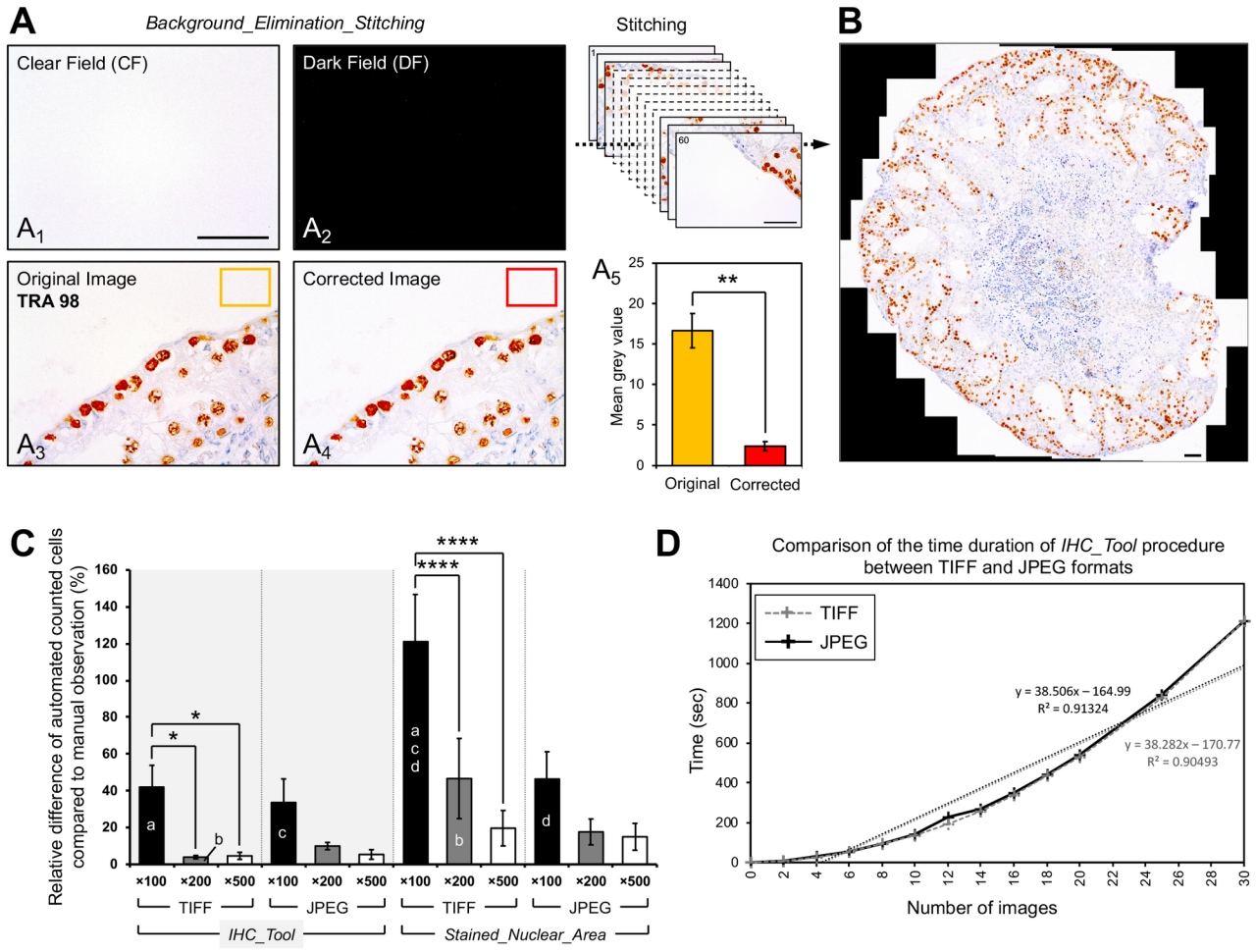
A
Background_Elimination_Stitching
Clear Field (CF)
A1
Dark Field (DF)
A2
Stitching
1
60
B
Original Image
TRA 98
A3
Corrected Image
A4
A5
Mean grey value
**
Original
Corrected
C
Relative difference of automated counted cells compared to manual observation (%)
****
****
*
*
a
b
c
a c d
b
d
×100 ×200 ×500 ×100 ×200 ×500 ×100 ×200 ×500 ×100 ×200 ×500
TIFF
JPEG
TIFF
JPEG
IHC_Tool
Stained_Nuclear_Area
D
Comparison of the time duration of IHC_Tool procedure between TIFF and JPEG formats
TIFF
JPEG
y = 38.506x – 164.99
R² = 0.91324
y = 38.282x – 170.77
R² = 0.90493
Time (sec)
Number of images

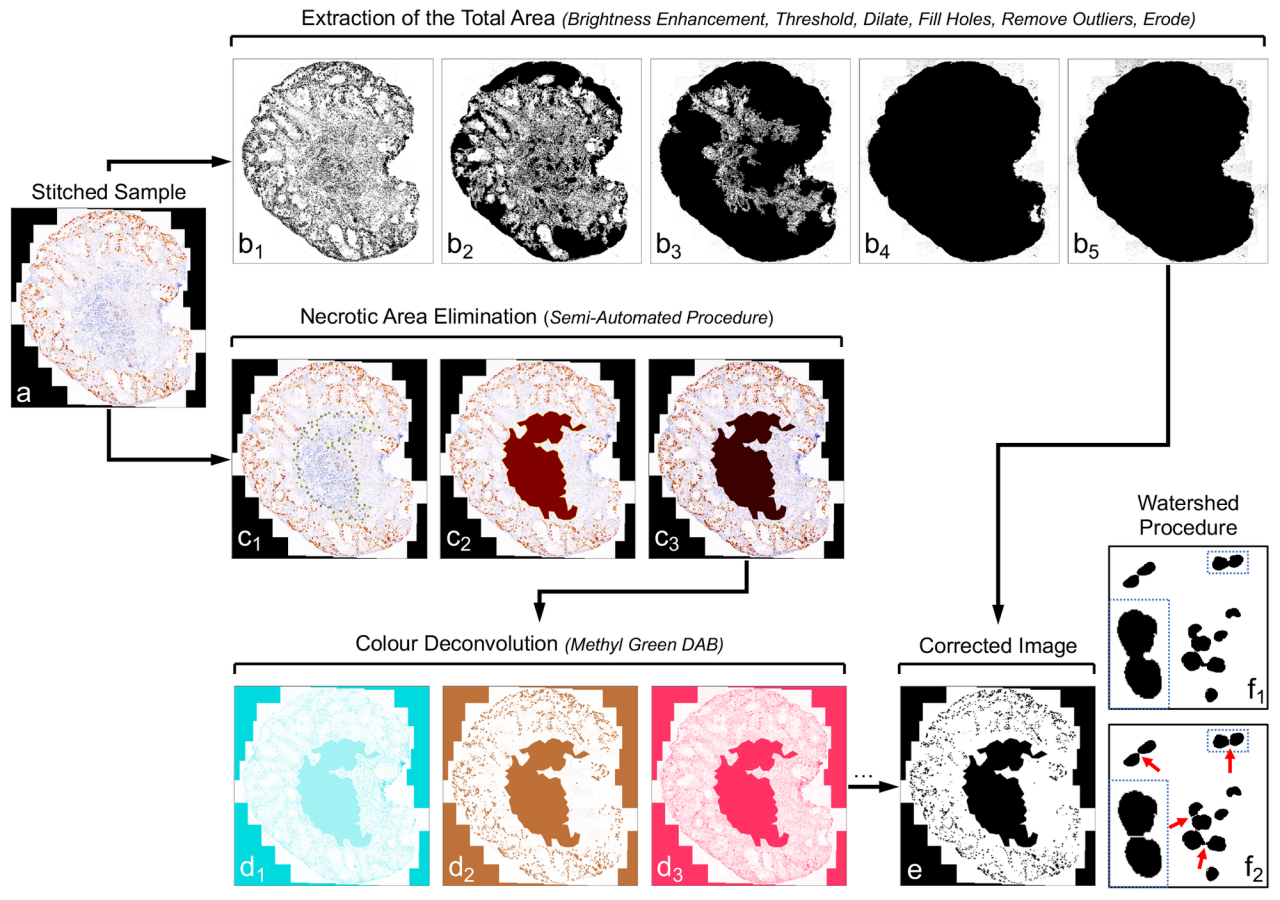
Extraction of the Total Area (Brightness Enhancement, Threshold, Dilate, Fill Holes, Remove Outliers, Erode)
Stitched Sample
a
b1
b2
b3
b4
b5
Necrotic Area Elimination (Semi-Automated Procedure)
c1
c2
c3
Colour Deconvolution (Methyl Green DAB)
d1
d2
d3
Corrected Image
e
Watershed Procedure
f1
f2